HHS Public Access

Author manuscript

ACS Sens. Author manuscript; available in PMC 2023 April 10.

Published in final edited form as:

ACS Sens. 2017 October 27; 2(10): 1458–1466. doi:10.1021/acssensors.7b00396.

Development of an Inexpensive RGB Color Sensor for the Detection of Hydrogen Cyanide Gas

Lee A. Greenawald[*,†], **Gerry R. Boss**[‡], **Jay L. Snyder**[#], **Aaron Reeder**[‖], **Suzanne Bell**[⊥]

[†]National Institute for Occupational Safety and Health, National Personal Protective Technology Laboratory, Evaluation and Testing Branch (CDC/NIOSH/NPPTL/ETB), Centers for Disease Control and Prevention, 1095 Willowdale Road, Morgantown, West Virginia 26505, United States

[‡]Department of Medicine, University of California, San Diego, 9500 Gilman Drive, La Jolla, California 92093, United States

[‖]National Institute for Occupational Safety and Health, National Personal Protective Technology Laboratory, Evaluation and Testing Branch (CDC/NIOSH/NPPTL/ETB), Centers for Disease Control and Prevention, 626 Cochrans Mill Road, Pittsburgh, Pennsylvania 15236, United States

[⊥]C. Eugene Bennett Department of Chemistry, West Virginia University, 217 Clark Hall, Morgantown, West Virginia 26506, United States

Abstract

An inexpensive red, green, blue (RGB) color sensor was developed for detecting low ppm concentrations of hydrogen cyanide gas. A piece of glass fiber filter paper containing monocyanocobinamide [CN(H_2O)Cbi] was placed directly above the RGB color sensor and an on chip LED. Light reflected from the paper was monitored for RGB color change upon exposure to hydrogen cyanide at concentrations of 1.0–10.0 ppm as a function of 25%, 50%, and 85% relative humidity. A rapid color change occurred within 10 s of exposure to 5.0 ppm hydrogen cyanide gas (near the NIOSH recommended exposure limit). A more rapid color change occurred at higher humidity, suggesting a more effective reaction between hydrogen cyanide and CN(H_2O)Cbi. The sensor could provide the first real time respirator end-of-service-life alert for hydrogen cyanide gas.

Graphical Abstract

[*]**Corresponding Author**: lgreenawald@cdc.gov. Phone: 304-285-5932.

[#]Present Address: 113 Snee Drive, Jefferson Hills, PA, 15025, United States

Author Contributions

The manuscript was written through contributions of all authors. All authors have given approval to the final version of the manuscript. These authors contributed equally.

The findings and conclusions in this report are those of the authors and do not necessarily represent the views of the National Institute for Occupational Safety and Health. Mention of product name does not constitute endorsement by the National Institute for Occupational Safety and Health or the Centers for Disease Control and Prevention.

The authors declare no competing financial interest.

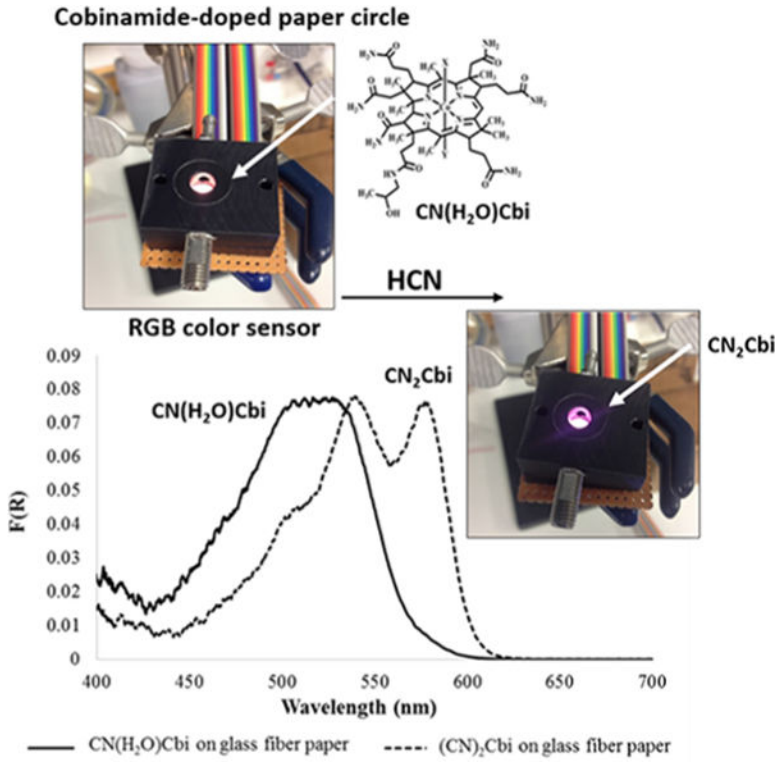

Keywords

cobinamide; hydrogen cyanide; paper-based sensor; respirator; end-of-service-life indicator

Air-purifying respirators are worn in occupational settings to protect the worker when the air is contaminated with harmful gases, aerosols, or vapors. Unfortunately, the user generally does not know when to change a canister/cartridge before breakthrough occurs—i.e., when the activated carbon is sufficiently saturated such that a harmful amount of the contaminant may penetrate the canister/cartridge.[1] Software models generated by respirator manufacturers are used to help estimate when breakthrough will occur, but the user may not be aware of unpredictable input data such as types and concentrations of toxic chemicals, relative humidity, and breathing rate. Additionally, most software models were developed for organic vapors.

In 1984, the National Institute for Occupational Safety and Health (NIOSH) published standards for certifying active end-of-service-life indicators (AESLI) to encourage development of sensors that can indicate imminent breakthrough.[2] The standards require that the sensors be embedded in a respirator carbon bed and provide a real-time alert (e.g., flashing light emitting diode (LED)) when the cartridge is near sufficient saturation to cause imminent vapor breakthrough. Current challenges in developing respirator cartridge sensors are the effects of humidity, selectivity, size, weight, and power restrictions. Additionally, manufacturers prefer to limit sensor costs to about $1 per cartridge, and $20–$50 for sensor-related fixtures and electronics.[2] Only a limited number of colorimetric and qualitative end-of-service-life indicators (ESLI) are commercially available, e.g., for organic vapor;

these rely on subjective visual identification of a color change.[3] For passive ESLIs, the user must routinely monitor the sensor for color change. This is inappropriate in poorly lit environments, in full facepiece respirators that may become fogged, or for color-blind persons. Currently, no NIOSH-approved AESLIs exist.

We have previously shown that diffuse reflectance of cobinamide—a vitamin B_{12} derivative—immobilized on cellulose and glass fiber filter paper is an effective and inexpensive AESLI prototype for detecting hydrogen cyanide (HCN) and hydrogen sulfide (H_2S) gas.[4,5] However, miniaturization and fabrication of spectrometers may be difficult and expensive. Color sensors are an economical and easily miniaturized alternative, where light is separated into a set of colors, primarily red (R), green (G), and blue (B).[6] Modern color sensors are used to assess pH, and to quantify color in the food, beverage, cosmetic, printing, and textile industries.[6,7] Many color sensors do not function in real-time—i.e., the sensor is exposed to the analyte and scanned (via flatbed scanner) into a computer, which is not realistic for a respirator ESLI application. The color analysis is performed by software (e.g., Adobe Photoshop) or on a smartphone application in terms of RGB values of 8-bit resolution (256-bit color scale with 255, 255, 255 corresponding to white, and 0, 0, 0 corresponding to black).[8,9] Data are frequently presented in terms of total color differences (ΔC) using the Euclidean distance equation:[9,10]

$$\Delta C = \sqrt{(\Delta R)^2 + (\Delta G)^2 + (\Delta B)^2} \quad (1)$$

where ΔR, ΔG, and ΔB are the change in R, G, and B colors from reference values, respectively.

We chose HCN gas to assess proof-of-concept of an RGB color sensor and compare it to a previously reported diffuse reflectance configuration which comprised a tungsten halogen light source, miniature spectrometer, and bifurcated optical fiber (herein referred to as the “diffuse reflectance configuration”).[4] Hydrogen cyanide has a NIOSH short-term recommended exposure limit (REL) of 4.7 parts-per-million (ppm) HCN; this means a worker should not inhale HCN concentrations above 4.7 ppm during a 15 min time-weighted average exposure at any time during a 10 h work day. A HCN ESLI located in the back end of a respirator canister must be able to rapidly detect a minimum 4.7 ppm of HCN. Paper is a unique substrate for real-time, low cost sensors because paper offers a bright, high-contrast backing and is highly porous, an advantage for rapid adsorption of gas phase analytes. We chose cobinamide (Cbi) as the indicating compound to detect HCN; it can bind up to two cyanide (CN^-) ions with an overall affinity of $K_a = 10^{22}$ M^{-2}.[11] The Cbi structure is shown in Figure S1 (Supporting Information), where the X and Y ligands can be OH^-, H_2O, HS^-, or CN^-, among others. At neutral pH in water, Cbi exists as the mixed aquo-hydroxo complex $OH(H_2O)$Cbi, termed aquohydroxocobinamide (with Co in 3+ oxidation state).[12] Adding a 1:1 mol equiv of CN^- to $OH(H_2O)$Cbi produces $CN(H_2O)$Cbi (monocyanocobinamide), which on binding a second cyanide ion provides fast and sensitive detection of cyanide forming CN_2Cbi (dicyanocobinamide), with resulting characteristic spectral shifts and a visible color change.[12,13]

The RGB sensor developed is enclosed in a light-tight holder, allowing a CN(H_2O)Cbi-immobilized paper circle to be exposed to HCN gas. The sensor is regulated by a microcontroller, which converts data to real time RGB readouts and allows for rapid color change analysis. Color change was monitored as a function of HCN concentration, time, and percent relative humidity (%RH). We compared the RGB color sensor, a diffuse reflectance configuration, and a commercially available electrochemical detector to monitor HCN breakthrough of respirator canisters.[4]

MATERIALS AND METHODS

Chemicals and Materials.

Aquohydroxocobinamide [OH(H_2O)-Cbi], Co(III) was synthesized from hydroxocobalamin as described previously.[14] A benchtop UV–vis spectrometer (Thermo Scientific Evolution 300) was used to verify the CN(H_2O)Cbi solution concentration under the following conditions: pH = 7.0 in deionized H_2O; 1.0 cm path length; molar extinction coefficient of 10,450 M^{-1} cm^{-1} at 583 nm.[15] Potassium cyanide (KCN) was purchased from Fisher Scientific (granular; certified ACS) and dissolved in 1 M sodium hydroxide (NaOH; (Fisher Scientific, certified). Stock HCN gas was purchased from Butler Gas at a concentration of 495.0 (±2%) ppm. Gelman Sciences A/E Borosilicate glass fiber filter paper (without binder, 330 μm thick, 1 μm pore size) was used as the support media. Deionized water was from an 18 MΩ-cm deionized in-line water system (Thermo Scientific Micropure).

Preparation of Paper Substrates.

Glass fiber filter paper was cut into uniform 6.0 ± 0.5 mm diameter circles. CN(H_2O)Cbi was pipetted onto the paper circles and allowed to dry fully (~1 h). The CN(H_2O)Cbi concentration was optimized by comparing color change after pipetting 15.0 μL of 50.0, 100.0, 200.0, and 300.0 μM CN(H_2O)Cbi before and after exposure to 5.0 ppm of HCN. The selected CN(H_2O)Cbi concentration was compared across 30 samples using the RGB sensor, along with RGB values for 12 blank samples. Data were analyzed by the average of each R, G, and B value using standard deviation (SD), relative standard deviation (%RSD), and 95% confidence interval (CI).

RGB Color Sensor and Test Holder.

An RGB color sensor chip (TCS34725, ams) was purchased from Adafruit (adafruit.com).[16] The chip incorporates the sensor along with a neutral white, 4150 K LED to illuminate the material of interest (Figure 1).[16]

The photodiode color array comprises a 4 × 3 array of red, green, and blue-filtered photodiodes, as well as three clear (unfiltered) photodiodes. Four integrated analog-to-digital (ADC) converters simultaneously convert the amplified photodiode currents to a 10-bit digital value.[16] The results are then transferred to data registers and communicated to a microcontroller through a 400 kHz, Inter-Integrated Circuit (I^2C) serial bus.[16] The LED is indium gallium nitride (InGaN) based, and has a viewing angle of 120°, with maximum illumination in the desired spectrum ranges (400–700 nm).[16] An infrared (IR) blocking filter is integrated on the chip and located near the color sensing photodiodes. The manufacturer

reports that this minimizes the IR spectral component and allows more accurate color measurements.[16]

Header pins were soldered directly onto the backside of the chip to ensure efficient electrical contact when connecting to a ribbon cable (Figure S2A). A ribbon cable was soldered to the sensor pins and used to connect the RGB sensor to appropriate ports on the Arduino microcontroller (Figure S2B and C). The microcontroller was connected to a laptop via universal serial bus (USB) cable and controlled with software using I^2C communication. Color View software sketch was used to control the color sensor and provide output data in separate R, G, B, and clear light elements. Sensor output values, separated by RGB values, are in terms of counts or digital values (D.V.; particularly counts/$\mu W/cm^2$). The sketch was modified to output RGB values at 6 s intervals, and calculate the total change in color (ΔC) at each measurement using eq 1. The sensor can be modified to indicate when a minimum ΔC is reached by flashing the LED (to simulate reaching end-of-service-life; Figure S2D).

A test holder housed the RGB sensor (Figure S2D). The holder incorporates a glass window separating HCN from the sensor electronics, while allowing HCN to flow over the Cbi-immobilized glass fiber paper. A complete assembly can be seen in Figure S2E. Light is reflected from the paper circle and detected by the color sensor photodiodes. ΔC is computed by the microcontroller program using eq 1.

System Optimization.

When light is detected by the photodiodes, current is generated that is converted to voltage and separated into respective R, G, and B output values in the form of digital values (D.V.). A sensor clock runs at 425 Hz, or 2.4 ms, the lowest possible single integration time for this configuration. The chip uses a 10-bit ADC, and the sensor has a 3,800,000:1 dynamic range, with adjustable integration time (2.4–700 ms) and gain for increased sensitivity.[16] An integration time of 700 ms yields 256 cycles, or 65,535 maximal counts (i.e., 16-bit resolution). ΔC values were computed every 6 s based on initial RGB values for $CN(H_2O)$Cbi calculated by eq 1.

Chip-LED and Color Sensor Responsivity.

A previously described diffuse reflectance configuration comprising a bifurcated optical fiber, Ocean Optics miniature spectrometer, and tungsten halogen light source was used here to determine the normalized intensity of the chip-LED.[4,5] The common end of the bifurcated fiber optic was held close to the LED at different angles, to capture the average LED spectrum ($n = 3$) by the spectrometer. Spectral responsivity of the on-chip LED was determined by holding a mirror directly above both the chip-LED and photodiodes and recording the RGB values.

Experiments were performed to ensure the chip-LED did not degrade or alter the Cbi spectrum when the paper is placed in the holder and exposed to the LED. Using the diffuse reflectance configuration, an initial Kubelka–Munk reflectance (in terms of the remission function, F(R)) spectrum was taken and the paper circle was inserted into the RGB color sensor holder for 60 min ($n = 3$; LED on). Final F(R) spectra were taken immediately after

using the same diffuse reflectance configuration. Total ΔC after 60 min was calculated (n = 6).

To determine ΔC drift in the absence of HCN, samples were placed in the sensor holder for 30 min with the desired %RH (25%, 50%, or 85%). Reference R (i.e., R_1), G (i.e., G_1), and B (i.e., B_1) values were recorded at t = 0. ΔC values were obtained every 6 s. Average ΔC values (in triplicate) were evaluated for each %RH.

HCN Flow Experimental Setup: NIOSH REL.

A low HCN concentration gas-flow experimental setup is shown in Figure S3 and was described previously.[4] Three mass flow controllers (MFCs; Alicat Scientific) regulate air flow, HCN concentration, and the percent relative humidity (%RH) based on air passing through a water bubbler. The HCN was diluted with oil-free compressed air and the concentration was confirmed using an HCN-specific electrochemical detector (Interscan RM, 0–50.0 ± 0.1 ppm). The lowest HCN concentration that could be measured accurately was 1.0 ppm of HCN. All tubing was made of Teflon (PFTE) material. Experiments were performed at a carrier gas flow rate of 0.75 L per minute (LPM) at 25%, 50%, and 85% RH at room temperature. This flow rate prevents back pressure in the sensor holder, and although it does not correlate with air flow through a respirator canister/cartridge, it was chosen to focus on studying the ΔC for the reaction between HCN and CN(H_2O)Cbi. The small size of the sensor holder combined with the 0.75 LPM flow rate yields a several second time constant for a step change in HCN concentration.

The system was flushed with air at the desired %RH (no HCN) for 1–2 h. A piece of CN(H_2O)Cbi-immobilized paper was then placed in the test holder and the initial RGB values (pre-HCN exposure) were recorded. The paper circles were allowed to equilibrate with the desired %RH for 15 min, and once the desired HCN concentration was detected by the electrochemical detector, a three-way valve was switched to direct air through the test holder, above the CN(H_2O)-Cbi-immobilized paper circle. The valve switching time was designated as the start of the experiment (i.e., t = 0). The CN(H_2O)Cbi paper was then exposed to HCN concentrations of 1.0, 3.0, 5.0, and 10.0 ppm, where ΔC was calculated using RGB values recorded at t = 0, 1, 5, 10, and 15 min after HCN exposure (n = 3 for each concentration). The R, G, B values at t = 0 are the reference values (i.e., R_1, G_1, B_1) after equilibration.

HCN Flow Experimental Setup: HCN Breakthrough of Respirator Canisters.

HCN breakthrough experiments were performed at the NIOSH, National Personal Protective Technology Laboratory (NPPTL) facility in Pittsburgh, PA. The standard test procedure (STP) with associated experimental equipment and setup titled “Determination of CBRN Acid Gases (Hydrogen Cyanide) Service-Life Test, Air-Purifying Standard Test Procedure (STP-CET-APRS-STP-CBRN-0303)” can be found online.[17] In short, an Interscan electrochemical HCN detector was placed downstream of the respirator canister to sample effluent flow and monitor HCN breakthrough from NIOSH-approved Chemical, Biological, Radiological, and Nuclear (CBRN) canisters used to provide protection against HCN. This downstream electrochemical detector was calibrated with certified 10.1 ppm of

HCN (±5%). To verify the challenge gas concentration, a Photoacoustic Multi-Gas Monitor 1314A (California Analytical Instruments Model UA989) with an optical filter for HCN was used. This instrument samples gas at 30 mL/min (±1% of measured value); range for HCN is (0.8–8000) ± 0.08 ppm. This instrument was calibrated with certified 1001 ± 2% ppm of HCN calibration gas. All valves were controlled by a custom LabVIEW based software. Average %RH, temperature, challenge HCN concentration (photoacoustic gas monitor), breakthrough concentration (electrochemical detector), and test time were monitored and stored by the software in real time. The high concentration gas-flow experimental setup can be seen in Figure S4. The canisters were mounted on a fixture within the airtight testing chamber. One opening located on the side of the test chamber was used for entry of the challenge gas, where exit gas is forced through the canister and through an outlet in the back of the test chamber, where the effluent gas is sampled by the downstream detector.[17]

The system was initially flushed with clean, oil-free air at 64 LPM at the desired %RH (no HCN) for 30 min, and then evaluated by the electrochemical detector to ensure a reading of 0.0 ppm of HCN. Air was pulled through the test holder in the diffuse reflectance configuration at 1.0 LPM (±5%) and through the RGB color sensor holder at 0.75 LPM (±5%) by a Gilian Air Sampling Pump (GilAir-3, Figure S6). The tubing from the test chamber to each sensor holder was 1.2 m long, permitting a time delay of 2.3 s. A piece of CN(H_2O)Cbi-impregnated paper was then placed in each holder; the initial reflectance spectrum was recorded, along with the initial RGB values. The diffuse reflectance spectrum of CN(H_2O)Cbi-immobilized paper was designated as the “blank” to monitor changes in the CN(H_2O)Cbi spectrum. Diffuse reflectance spectra and RGB values were recorded at various time intervals throughout each experiment and at HCN breakthrough.

To determine if distinguishable Cbi spectral shifts were a result of a cyanogen byproduct due to reaction of HCN with the activated carbon chemical impregnants, a Kin-TEK Trace Source cyanogen permeation tube was used to expose 5.0 ± 2% $(CN)_2$ over the Cbi paper sensor at 0.49 ± 0.01 LPM at 30.00 ± 0.01 °C by using the following permeation tube calculator:

$$C_{\text{ppmv}} = \frac{E_{\text{ng/min}} \times 22.41}{\text{MW} \times F_{\text{pd}}} \quad (2)$$

where C_{ppmv} is the generated concentration (ppm by volume), $E_{\text{ng/min}}$ is the emission rate of component from the permeation tube, MW is the molecular weight of the component (g/mol), 22.41 is the volume (L) of 1 mol of gas at standard temperature and pressure, and F_{pd} is the primary dilution flow rate (standard cubic centimeters, sccm). The cyanogen permeation tube was stored within a heated Kin-Tek Flexstream Gas Standards Generator. The flow rate was set to generate 5.0 ± 0.1 ppm cyanogen at an emission rate of 5837 ng/min at 30 °C.

RESULTS AND DISCUSSION

Volume and Concentration of Cobinamide.

In previous studies, glass fiber filter paper demonstrated larger reflectance signals than cellulose filter paper, presumably because the glass fiber paper is thicker and allows more light to reach the detector in a reflectance configuration.[4,5] Additionally, glass fiber paper is less affected by water vapor. The optimal concentration and volume of $CN(H_2O)Cbi$ placed on the paper was found to be 15.00 ± 0.02 μL of 200.0 ± 0.2 μM. This volume and concentration of $CN(H_2O)Cbi$ was pipetted onto the center of each piece of paper leading to ~3.6 μg $CN(H_2O)Cbi$ per paper circle. The $CN(H_2O)Cbi$ solution diffused uniformly across the paper circle, and the wetted paper was allowed to dry fully for 1 h at room temperature (~21 °C). These optimized conditions yielded a reflectance spectrum with subjectively acceptable signal-to-noise ratio without being too concentrated, which would result in lower sensitivity in determining small color changes. The spotted papers were stored at 4 °C. The average RGB values of blank (n = 12) and 200 μM Cbi-immobilized paper (n = 30) are shown in Table S1.

UV–vis Spectra of Cobinamide.

The absorbance spectra of 20 μM $OH(H_2O)Cbi$, $CN(H_2O)Cbi$, and $(CN)_2Cbi$ in aqueous solution are shown in Figure 2A. When a second cyanide ion binds to $CN(H_2O)Cbi$, a peak appears at 583 nm, absorption at 450–500 nm decreases, an isosbestic point occurs at 531 nm, and a visible violet color develops. The absorption spectrum of a 50 μM $CN(H_2O)Cbi$ solution is similar to the optical fiber diffuse reflectance spectra of $CN(H_2O)Cbi$ on glass fiber paper before and after excess CN^- (Figure 2B), indicating the binding of gas-phase CN^- is successful.

Effect of LED and Drift on Cbi Spectra.

The average (n = 3) normalized intensity spectrum of the chip-LED is shown in Figure S5. The warm neutral white LED emits a similar spectra shown in the manufacturer datasheet with a distinctive InGaN LED peak observable at ~450 nm.[16] When a mirror is placed directly above the chip-LED and photodiodes, the RGB values are recorded and normalized to the highest R (615 nm), G (525 nm), or B (465 nm) value. The spectral response using a mirror, blank glass fiber paper, and $CN(H_2O)Cbi$-immobilized glass fiber paper were similar at 465, 525, and 615 nm. A similar normalization approach was performed for blank glass fiber response (n = 12) and 200 μM $CN(H_2O)Cbi$ on glass fiber paper (n = 30) with the data shown in Table S2. The normalized data suggest an appropriate spectral response of the photodiodes for the blank glass fiber paper and immobilized $CN(H_2O)Cbi$ within the wavelengths of interest.

The chip-LED did not alter the Cbi spectrum when the paper sensor was placed in the sensor holder for 1 h. Using the optical fiber diffuse reflectance setup, an initial F(R) spectrum for 200 μM $CN(H_2O)Cbi$-fixed paper was recorded, after which the paper circle was inserted into the RGB color sensor holder. The overall spectrum of $CN(H_2O)Cbi$ remained the same. The total average ΔC after 60 min of LED exposure was 195.6 ± 24.8 (uncertainty in 95% CI; n = 6) with data shown in Table S3.

Cobinamide Detection of HCN at the NIOSH REL Using the RGB Color Sensor.

A paper circle impregnated with $CN(H_2O)$Cbi was secured in the sensor holder and exposed to HCN gas. The average R, G, and B values after exposure to 5.0 ppm of HCN (close to the NIOSH HCN REL) at 25%RH are shown in Figure 3. The R (dotted line) and G (dashed line) values decreased, while the B values (solid line) increased as a function of time. The increase and decrease in readings correlate well with $(CN)_2$Cbi absorbance intensities—i.e., upon formation of $(CN)_2$Cbi, an absorbance increase occurs from 531 to 600 nm, while a decrease occurs from ~420 to 531 nm (Figure 2B). A decrease in absorbance in the blue region of $(CN)_2$Cbi absorption increases the reflectance/signal detected by the RGB color sensor, and thus an increase in the blue-filtered photodiode signal is observed. It would be possible to monitor just the ΔB, but the addition of ΔR and ΔG help compensate for drift and potential interfering gases—this will be further explored. ΔC was calculated using eq 1; the red photodiode displayed the largest response, followed by the G and B photodiodes with ΔC corresponding to 1910 ± 130, 880 ± 110, and 420 ± 30, respectively (uncertainty expressed by S.D.).

Detection at non-NIOSH REL HCN Concentrations.

Exposing the paper to 1.0, 3.0, and 10.0 ppm of HCN at 25% RH increased the ΔC as a function of HCN concentration, where exposure to 3.0 and 10.0 ppm cause the response to plateau after ~15 min (Figure 4A, $n = 3$). All concentrations at 25%RH had similar response curves, but yielded different final ΔC values and slopes; average initial ΔC values ($n = 3$) are in Figure 4B. The 25%RH blank is the average drift response of a $CN(H_2O)$Cbi paper exposed to 0.0 ppm of HCN air at 25%RH after 15 min of equilibration (final ΔC= 117.3 ± 66.6, $n = 3$). As reported earlier, the average ΔC drift after 60 min of 0.0 ppm of HCN at 25%RH was 195.6 ± 24.8; thus, the ΔC of the RGB color sensor exposed to 1.0 ppm of HCN after 15 min is 10× this drift. Data for each concentration at 25%RH are shown in Table S4.

Effect of Percent Relative Humidity (%RH) on HCN Detection.

Increasing the %RH to 50% increased the ΔC at all HCN concentrations compared to exposure to 25%RH. Total ΔC after 15 min for the R, G, and B photodiodes were 3100 ± 500, 1700 ± 500, and 790 ± 70, respectively. Average R, G, and B values for 5.0 ppm of HCN at 85%RH are shown in Figure 5A. Each color-filtered photodiode responds rapidly, with the signal reaching steady state within 2 min of HCN exposure. The plateau for the remainder of the experiment is stable. The total ΔC after 15 min for the R, G, and B photodiodes at 85% RH are 3600 ± 300, 1500 ± 100, and 900 ± 90, respectively ($n = 3$). The average computed total ΔC for each HCN concentration at 85%RH is shown in Figure 5B ($n = 3$), with data in Table S4. The increased ΔC may be attributed to water vapor adsorption by the paper, creating a more solution-like medium for CN^- binding to $CN(H_2O)$Cbi and thus allowing a more rapid reaction.

To assess reversibility, HCN was added to the gas stream at 0 and 30 min removed at $t = 15$ and 45 min (Figure 6). At each relative humidity, a small decrease in ΔC was observed when HCN was removed, which can be attributed to a slow, reversible removal of CN^- from the $(CN)_2$Cbi compound and a resultant color closer to that of the reference (i.e., $CN(H_2O)$Cbi

on paper). This demonstrated that the reaction is partially reversible in the gas-phase when CN^- is removed. For an ESLI, reversibility is not relevant as long as the user is alerted upon initial breakthrough and detection of the gas. In summary, high ΔC values are obtained by the RGB sensor as a function of increasing both the HCN concentration and/or % RH (Table S4). Steady-state conditions are reached rapidly at higher %RH, and thus the difference in ΔC values between 1 and 15 min exposure times at higher HCN concentrations is reduced.

HCN Canister Breakthrough Experiments: Diffuse Reflectance Configuration vs Electrochemical Detector.

A CBRN respirator canister was placed in the test fixture and exposed to a challenge concentration of 1000 ± 2% ppm of HCN until breakthrough was observed. A comparison of breakthrough curves for the Cbi paper using the diffuse reflectance configuration (primary axis) and the electrochemical detector (secondary axis) is shown in Figure 7 (the raw data from the electrochemical detector is shown in Figure S7A).

A small amount of HCN permeated through the carbon bed throughout the test as indicated by the diffuse reflectance configuration sensor. Small amounts of breakthrough commonly occurs during canister testing and may be due to low amounts of vapor permeating through the channels of the irregular carbon granules (common in high-flow canister testing) or the formation of chemical byproducts (e.g., cyanogen). However, an increase in the F(R) slope near 120 min is apparent and corresponds to canister breakthrough detected by the electrochemical detector near this time. A comparison of the first derivatives of the F(R) response at 583 nm and electrochemical response (raw data) shows that the start of breakthrough correlated well for both detectors with both sensors showing a change in slope, i.e., imminent breakthrough near 90 min (Figure S7B).

The ΔF(R) spectra at $t = 0$, 15, 30, 60, 105 min, and at the end of the test (164 min) are shown in Figure 8A. Distinctive spectral shifts for dicyanocobinamide are readily observed. The final concentration of HCN was ~1 ppm before the test was terminated (described in the Supporting Information). A small increase near 545 nm is observed along with less pronounced response from 450–500 nm compared to direct exposure of Cbi to HCN (expanded inset of Figure 8A). This difference could be due to generation of cyanogen [$(CN)_2$], an intermediate and/or byproduct of HCN removal by activated carbon.[18] Cyanogen is generated by oxidation of HCN in the presence of copper, a common impregnant in CBRN activated carbon.

The average Cbi F(R) spectrum after 10 min of 5.0 ppm $(CN)_2$ exposure and after 15 min of 5.0 ppm of HCN exposure are shown in Figure 8B ($n = 3$). When Cbi is exposed to $(CN)_2$, the distinctive dicyanocobinamide isosbestic point at 531 nm is not observed; however, the small increase near 545 nm observed during canister breakthrough experiments is apparent and the peak F(R) is slightly blue-shifted to shorter wavelengths (~568 nm), compared to 583 nm for exposure to HCN. Limited data are available for Cbi reaction with cyanogen. Because the absorbance spectrum of Cbi is dependent on the properties of the axial ligands to Cbi, the shift to shorter wavelengths may be due to the more electronegative donor ligand which tend to shift the peaks to shorter wavelengths.[19] The breakthrough data suggest that Cbi can detect small amounts of cyanogen produced as a byproduct of HCN exposure to

a respirator canister. This additive detection is important as the NIOSH REL of HCN is a summation of HCN and $(CN)_2$.

HCN Canister Breakthrough Experiments: Diffuse Reflectance Configuration vs RGB Color Sensor.

The RGB sensor was placed adjacent to the diffuse reflectance configuration test holder so that HCN breakthrough downstream of the respirator canister was detected simultaneously for both sensor configurations. ΔC (secondary-axis) of the RGB color sensor compared with the diffuse reflectance fiber optic configuration (ΔF(R), primary axis) is shown in Figure 9. The response for both sensors correlate well upon breakthrough of HCN.

At ~115 min, a change in slope is observed for both Cbi sensors. Similar to the diffuse reflectance configuration, the RGB sensor responds to low concentrations of HCN permeating through the canister as designated by the increase in ΔC prior to breakthrough. The cumulative response may cause a premature end-of-service life warning signal to a respirator user; thus more experiments are required to either lower the sensitivity or include an increased threshold. However, unrealistically high concentrations of HCN (i.e., 1000 ppm) were exposed to canisters during these breakthrough experiments (as per NIOSH testing protocols), so a minimized presence of HCN prior to breakthrough would be expected.

Other relevant gaseous species that bind to Cbi include hydrogen sulfide, ammonia, and nitric oxide. However, these species cause a spectral shift at wavelengths differently than the distinct spectral peak at 583 nm upon CN^- binding to Cbi.[5,14,19] Noncharged species (e.g., ethanol, toluene) bind poorly to cobinamide with spectral shifts dissimilar than the one at 583 nm; thus these species were not assessed in this proof-of-concept study, but will be further explored.[19]

CONCLUSION

An RGB color sensor is a promising low-power and inexpensive ESLI configuration to detect imminent breakthrough of a respirator. The amount of Cbi necessary to generate a color difference upon HCN exposure costs less than a penny per sample (assuming ~$1/mg Cbi). The RGB photodiodes demonstrated, in real-time, a rapid change in the red, green, and blue values of the $CN(H_2O)$Cbi compound on filter paper upon exposure to HCN at various concentrations and %RH levels. Total ΔC from initial $CN(H_2O)$Cbi on filter paper was calculated in real-time and yielded values that increased as a function of HCN concentration and %RH, where faster reaction kinetics may be attributed at higher %RH. Effects of temperature will be explored in future studies. Using the total ΔC values for each individual paper sensor decreases the variability between paper sensors. The RGB color sensor and associated electronics can be further miniaturized including use of microprocessing chips and Bluetooth technology. The RGB sensor also shows potential to detect low concentrations (ppb) of HCN and $(CN)_2$ through a respirator canister that correlated well with both a previously used fiber optic diffuse reflectance configuration and an HCN-specific electrochemical detector. The color sensor offers an economical and

quantitative approach to determine color-change of an end-of-service-life indicator and shows proof-of-concept for the first HCN ESLI.

Supplementary Material

Refer to Web version on PubMed Central for supplementary material.

ACKNOWLEDGMENTS

The authors acknowledge financial support from CDC, NIOSH NPPTL, and from the Office of the Director of NIH, and NINDS Grant #U01 NS058030 for the funding of this project. First author would like to acknowledge Drs. Nicole Fry, Dr. Michael Sailor, and Dr. Harry Finklea for insightful discussions that were essential to this manuscript. Author would also like to acknowledge Bradley Newbraugh (CDC, NIOSH DSR) for his assistance with the RGB color sensor electronic connections.

ABBREVIATIONS

NIOSH	National Institute for Occupational Safety and Health
AESLI	active end-of-service-life indicator
LED	light emitting diode
ESLI	end-of-service-life indicator
HCN	hydrogen cyanide
H_2S	hydrogen sulfide
R	red
G	green
B	blue
REL	recommended exposure limit
ppm	parts-per-million
Cbi	cobinamide
CN^-	cyanide ion
SD	standard deviation
% RSD	percent relative standard deviation
CI	confidence interval
D.V.	digital value
MFC	mass flow controller
LPM	liters per minute
NPPTL	National Personal Protective Technology Laboratory

CBRN	chemical, biological, radiological, nuclear
F(R)	diffuse reflectance

REFERENCES

(1). CDC End-of-Service-Life http://www.cdc.gov/niosh/npptl/topics/respirators/disp_part/RespSource3end.html (accessed 05/08/2015).

(2). Rose-Pehrsson S; Williams ML Integration of Sensor Technologies in Respirator Vapor Cartridges as End-of-Service Life Indicators: Literature and Manufacturers Review and Research Roadmap; 2005.

(3). 3M Worker Health & Safety http://www.3m.com/3M/en_US/worker-health-safety-us/personal-protective-equipment/organic-vapor-cartridge/ (accessed 07/20).

(4). Greenawald LA; Snyder JL; Fry NL; Sailor MJ; Boss GR; Finklea HO; Bell S Development of a Cobinamide-Based End-of-Service-Life Indicator for Detection of Hydrogen Cyanide Gas. Sens. Actuators, B 2015, 221, 379–385.

(5). Greenawald LA; Boss GR; Reeder A; Bell S Development of a hydrogen sulfide end-of-service-life indicator for respirator cartridges using cobinamide. Sens. Actuators, B 2016, 230, 658–666.

(6). Puiu PD Optical Nano-and Microsystems for Bioanalytics. In Springer Series on Chemical Sensors and Biosensors, Urban G, Ed.; Springer: Berlin, 2012; Vol. 10, pp 3–47.

(7). de la Torre C; Muñiz R; Peŕez MA A New, Lost-Cost, On-Line RGB Colorimeter for Wine Industry Based on Optical Fibers In XIX IMEKO World Congress, Portugal, 2009; pp 2554–2558.

(8). Janzen MC; Ponder JB; Bailey DP; Ingison CK; Suslick KS Colorimetric Sensor Arrays for Volatile Organic Compounds. Anal. Chem 2006, 78, 3591–3600. [PubMed: 16737212]

(9). Soga T; Jimbo Y; Suzuki K; Citterio D Inkjet-Printed Paper-Based Colorimetric Sensor Array for the Discrimination of Volatile Primary Amines. Anal. Chem 2013, 85, 8973–8978. [PubMed: 24044503]

(10). Eaidkong T; Mungkarndee R; Phollookin C; Tumcharern G; Sukwattanasinitt M; Wacharasindhu S Polydiacetylene paper-based colorimetric sensor array for vapor phase detection and identification of volatile organic compounds. J. Mater. Chem 2012, 22 (13), 5970–5977.

(11). Brenner M; Mahon SB; Lee J; Kim J; Mukai D; Goodman S; Kreuter KA; Ahdout R; Mohammad O; Sharma VS; Blackledge W; Boss GR Comparison of Cobinamide to Hyroxocobalamin in Reversing Cyanide Physiologic Effects in Rabbits using Diffuse Optical Spectroscopy Monitoring. Journal of Biomedical Optics 2010, 15, 017001. [PubMed: 20210475]

(12). Ma J; Dasgupta P; Zelder FH; Boss GR Cobinamide Chemistries for Photometric Cyanide Determination. A Merging Zone Liquid Core Wavequide Cyanide Analyzer Using Cyanoaquacobinamide. Anal. Chim. Acta 2012, 736, 78–84. [PubMed: 22769008]

(13). Baldwin DA; Betterton EA; Pratt JM The Chemistry of Vitamin B12. Part 20. Diaquocobinamide: pKa Values and Evidence for Conformatinal Isomers. J. Chem. Soc., Dalton Trans 1983, 217–223.

(14). Broderick KE; Singh V; Zhuang S; Kambo A; Chen JC; Sharma VS; Pilz RB; Boss GR Nitric Oxide Scavenging by the Cobalamin Precursor Cobinamide. J. Biol. Chem 2005, 280, 8678–8686. [PubMed: 15632180]

(15). Ford SH; Nichols A; Shambee M The Preparation and Characterization of the diaquo- Forms of Several Incomplete Corrinoids Cobyric Acid, Cobinamide, and Three Isomeric Cibinic Acid Pentaamines. J. Inorg. Biochem 1991, 41, 235–244. [PubMed: 2056308]

(16). Adafruit. Overview of Adafruit TCS34725; https://learn.adafruit.com/adafruit-color-sensors/overview (accessed 07/31/2015).

(17). NIOSH, Determination of CBRN Acid Gases (Hydrogen Cyanide) Service Life Test, Air-Purifying Respirators Standard Test Procedure (STP) NPPTL: Pittsburgh, 2005.

(18). Alves BR; Clark AJ An Examination of the Products Formed on Reaction of Hydrogen Cyanide and Cyanogen with Copper, Chromium (6+) and Copper-Chromium (6+) Impregnated Activated Carbons. Carbon 1986, 24 (3), 287–294.

(19). Pratt JM Inorganic Chemistry of Vitamin B_{12}; Academic Press Inc.: New York, 1972.

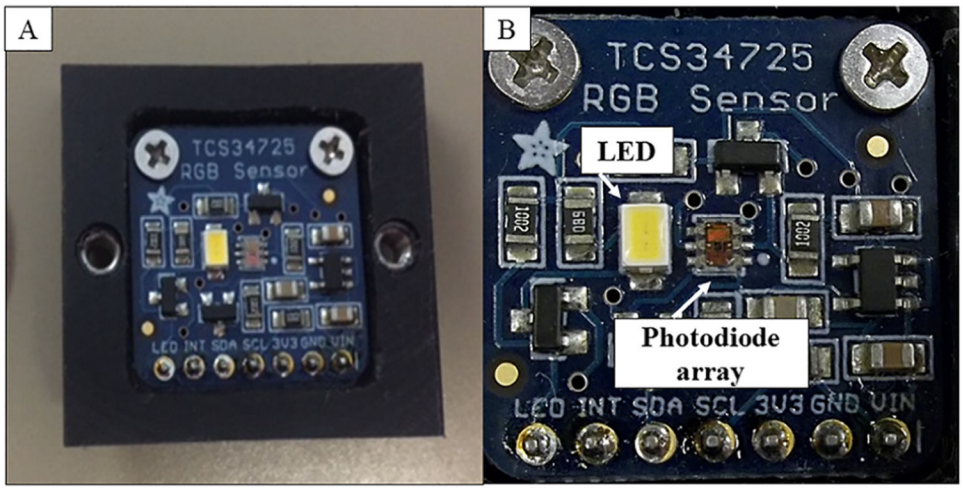

Figure 1.
(A) Top view of RGB color sensor in holder. (B) Expanded view of sensor chip.

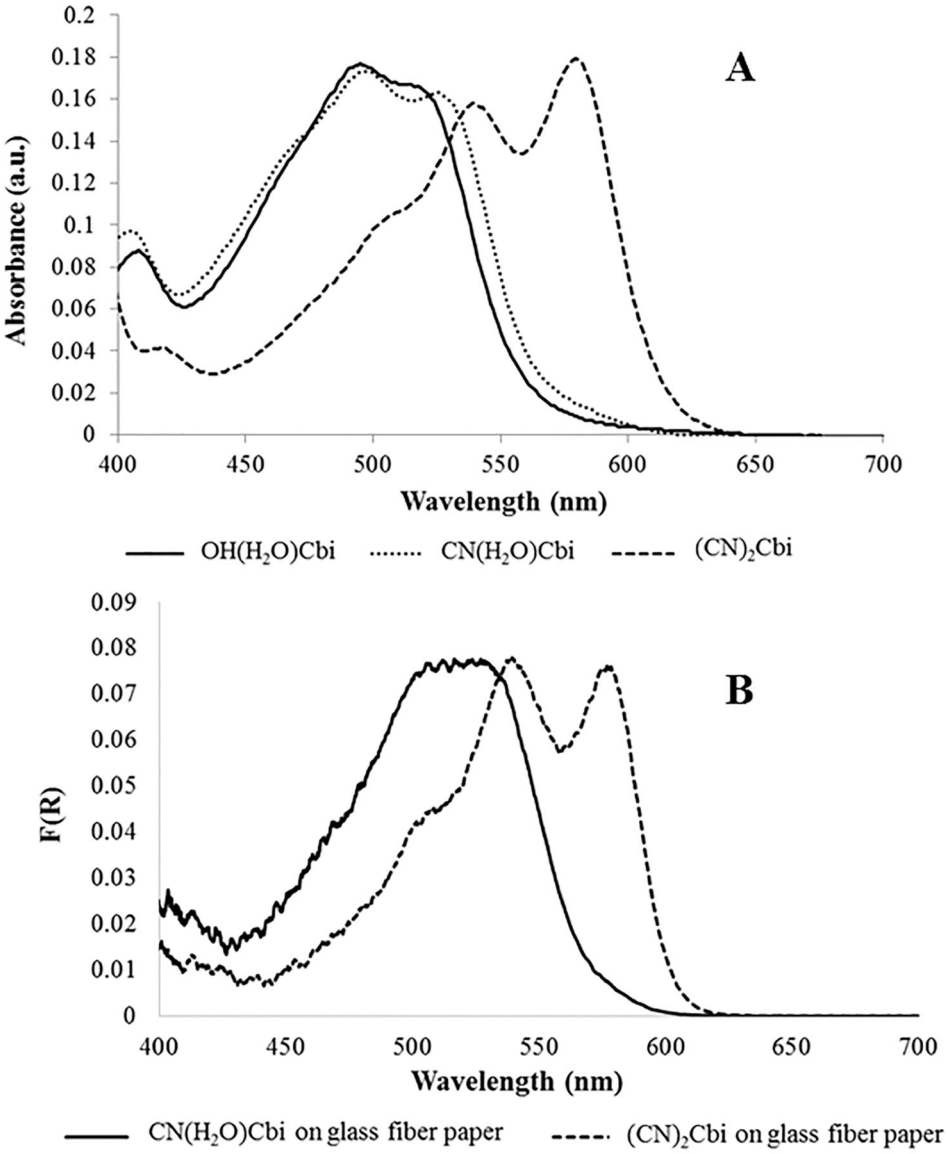

Figure 2.

(A) Absorption spectra of three Cbi complexes—20.0 μM $OH(H_2O)Cbi$ (solid line), 20.0 μM $CN(H_2O)Cbi$ (dotted line), and 20.0 μM $(CN)_2Cbi$ (dashed line).[4] (B) Diffuse reflectance spectra (plotted using the Kubelka–Munk function) of monocyanocobinamide on glass fiber paper before and after exposure to HCN. Part A reprinted with permission from ref 4. Copyright 2015, Elsevier.

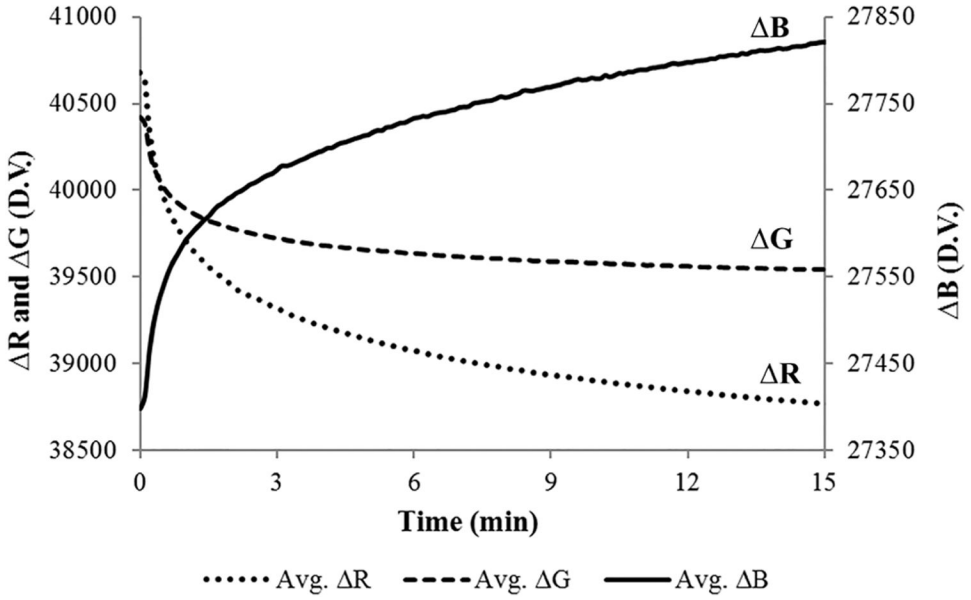

Figure 3.

Response of the separate Δ*R* (dotted line), Δ*G* (dashed line), and Δ*B* (solid line) values (D.V.) on exposure of CN(H_2O)Cbi-impregnated filter paper to 5.0 ppm of HCN at 25%RH.

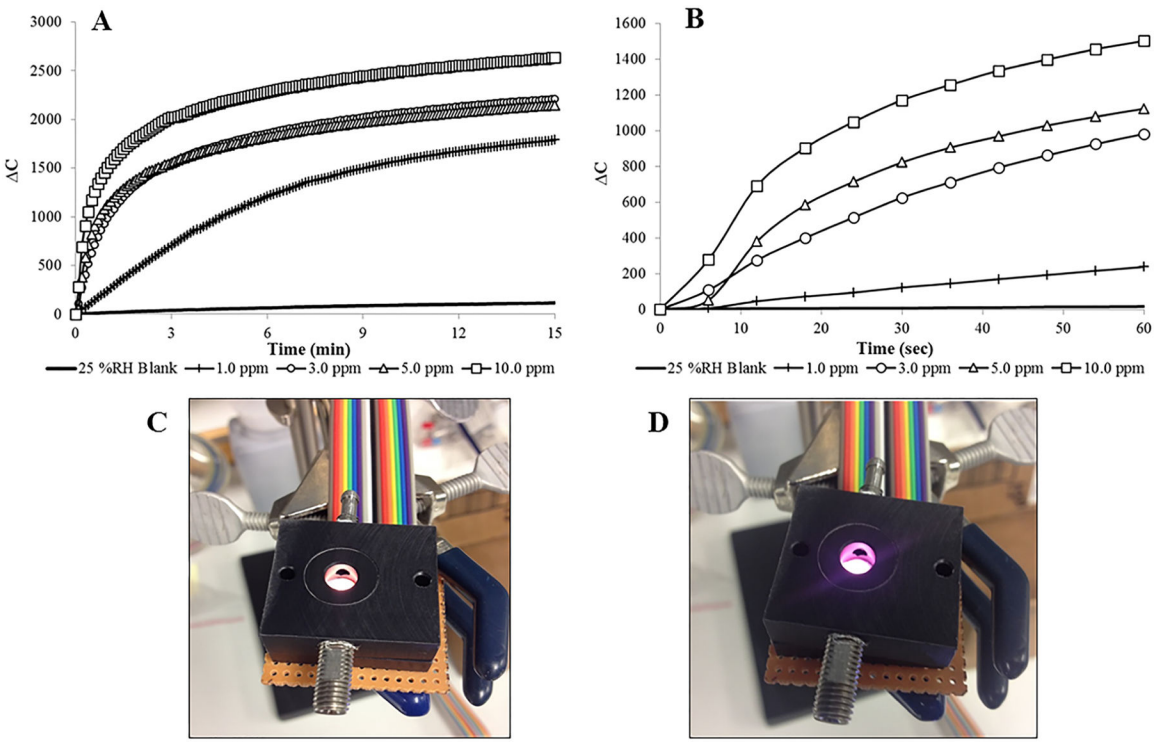

Figure 4.

(A) Total Δ*C* during HCN exposure of CN(H_2O)Cbi-impregnated filter paper at 25%RH–Blank (solid line), 1.0 ppm (crossed line), 3.0 ppm (circle line), 5.0 ppm (triangle line), 10.0 ppm of HCN (square line). (B) Expanded view of initial response (60 s). (C) CN(H_2O)Cbi on glass fiber filter paper after 10.0 ppm of HCN exposure with chip LED on and (D) before HCN exposure.

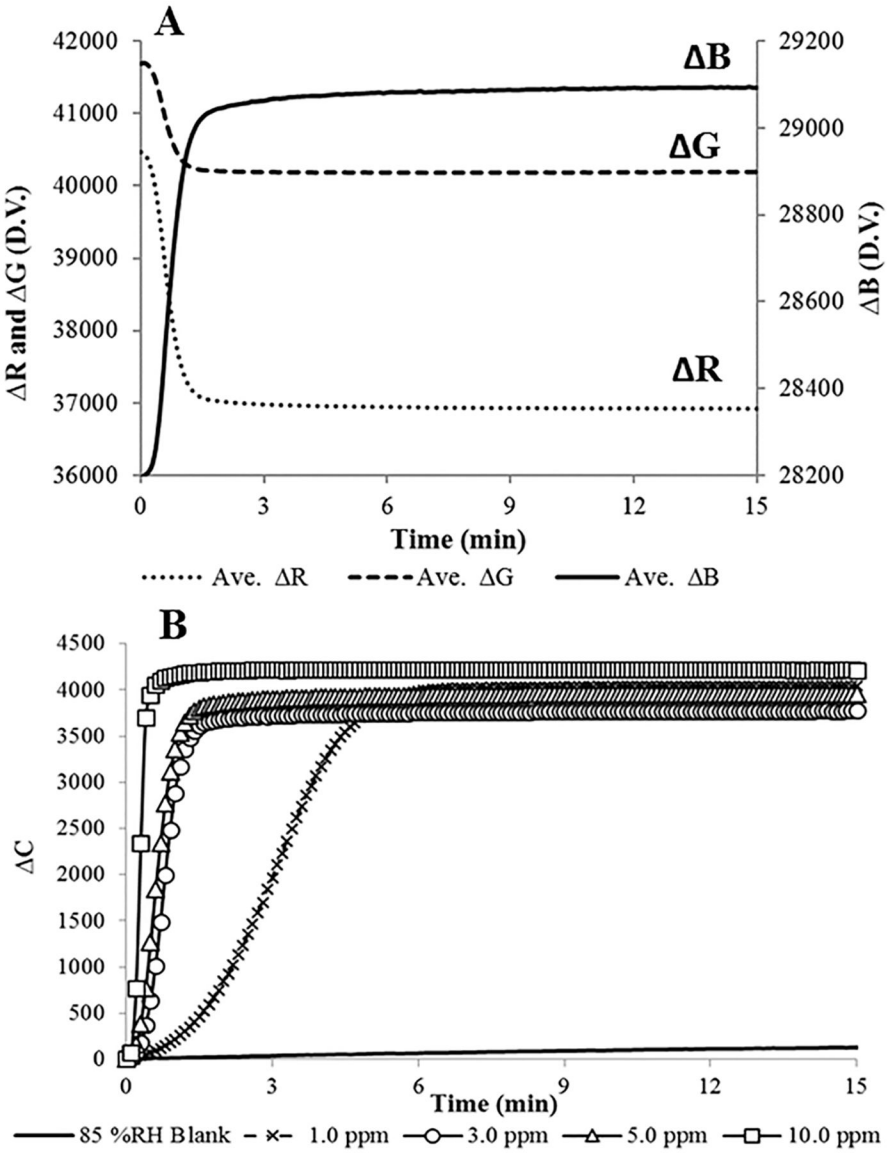

Figure 5.

(A) Response of the separate Δ*R* (dotted line), Δ*G* (dashed line), and Δ*B* (solid line) values (D.V.) upon 5.0 ppm of HCN exposure to the CN(H_2O)Cbi-impregnated filter paper at 85%RH. (B) RGB color sensor total Δ*C* during HCN exposure at 85%RH.

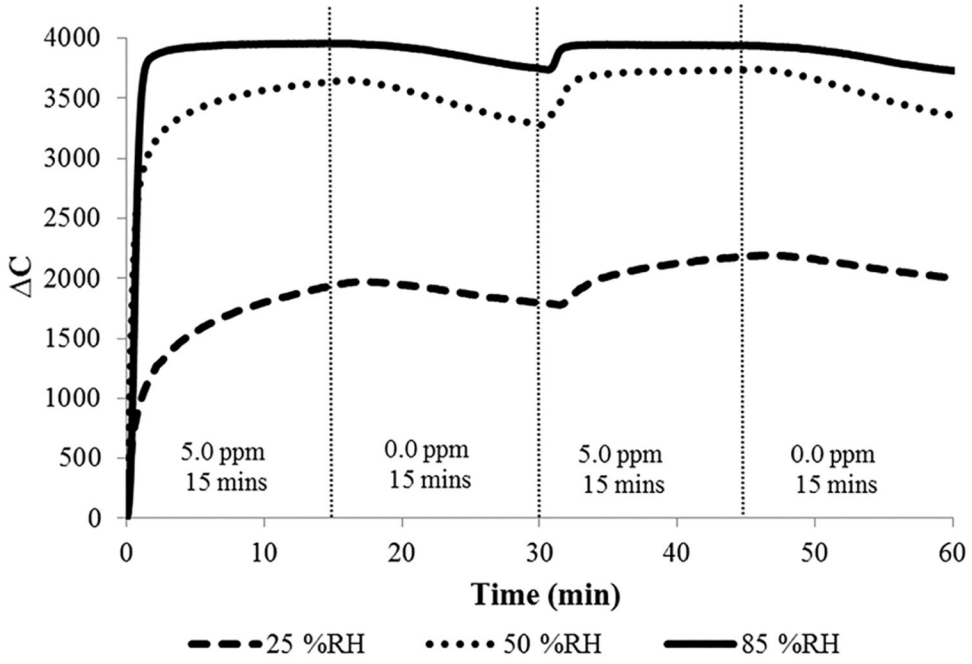

Figure 6.

Average total Δ*C* during 5.0 ppm of HCN exposure to the CN(H_2O)Cbi-impregnated filter paper at various %RH; HCN was cycled on and off (n = 3).

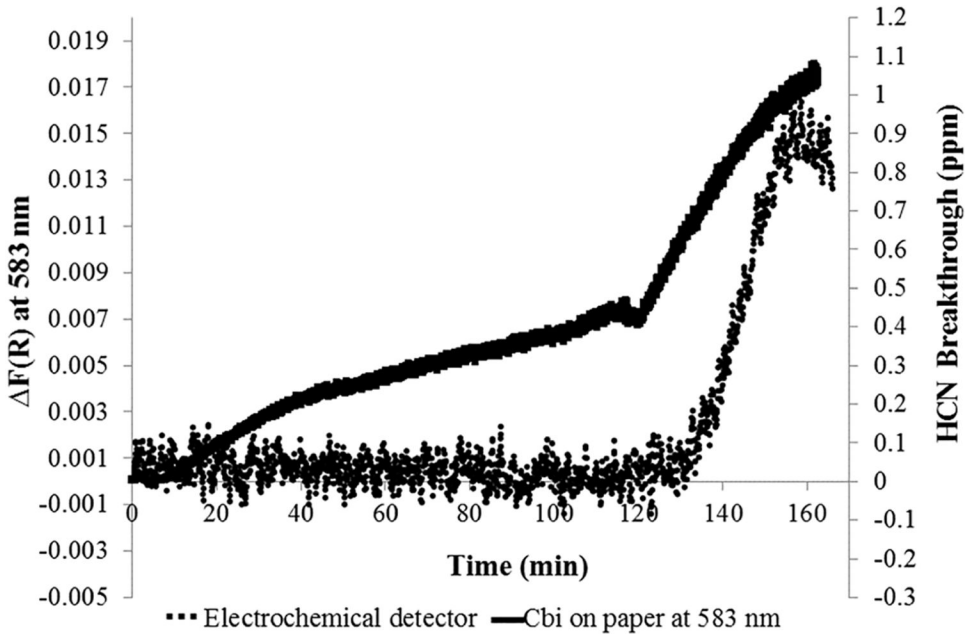

Figure 7.

Breakthrough curves for Cbi paper sensor at 583 nm (solid line) and electrochemical detector (dotted line; plotted as 10-point moving average). An average Cbi F(R) response of 700–750 nm is used as reference (not shown).

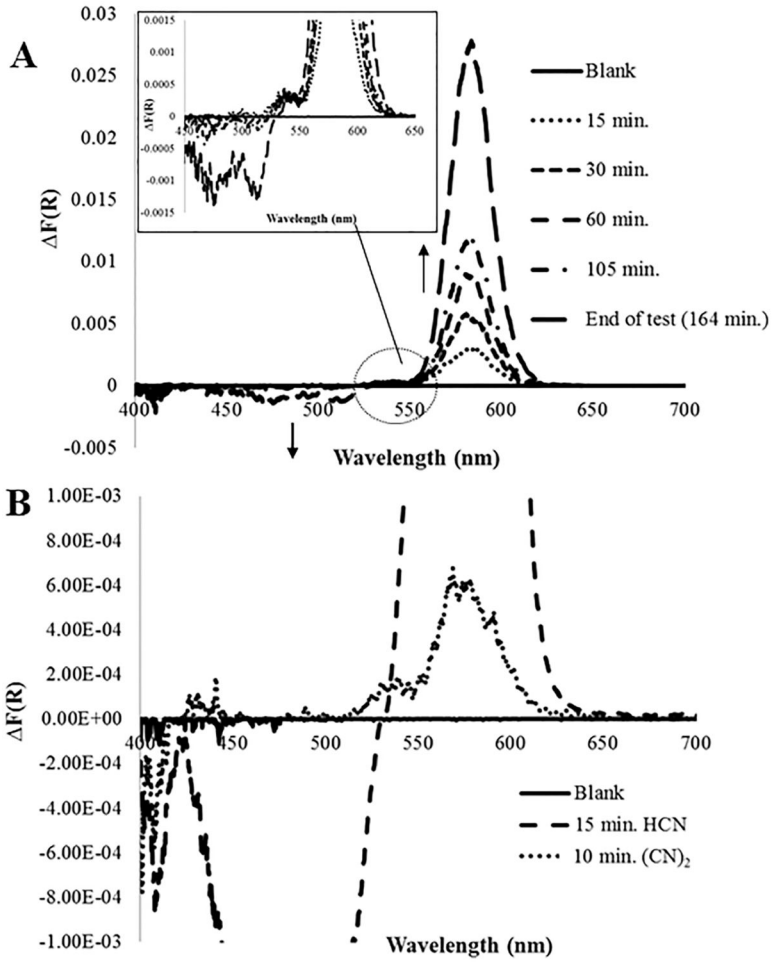

Figure 8.

(A) Δ*F*(R) spectra during HCN breakthrough experiment. Inset: Expanded view of 450–650 nm. (B). Comparison of $CN(H_2O)Cbi$ on paper when exposed to 5.0 ppm $(CN)_2$ and 5.0 ppm of HCN (separate experiments).

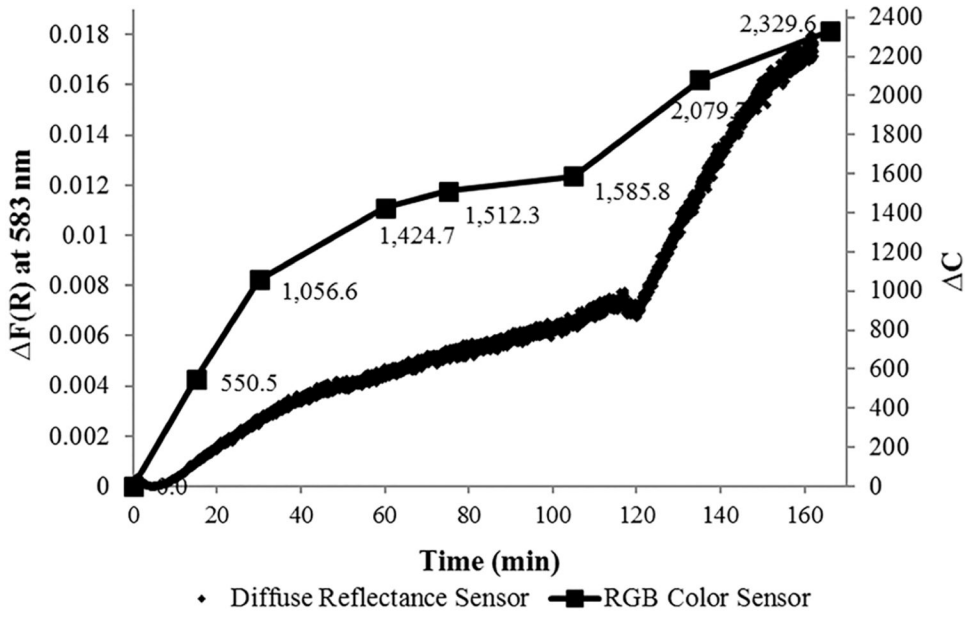

Figure 9.

$CN(H_2O)$Cbi-impregnated filter paper response to HCN breakthrough from a respirator canister using the RGB color sensor (square markers) compared to with the diffuse reflectance sensor configuration (diamond markers).